

Evaluation of mean performance of cracks bridged by multi-filament yarns

M. Konrad, J. Jeřábek, M. Vořechovský & R. Chudoba

Chair of Structural Statics and Dynamics, RWTH-Aachen University, Germany

This paper introduces an approach to modeling crack bridge behavior by evaluation of the mean performance of a multifilament yarn. The influence of imperfections in the material structure is discussed using several parametric studies. The disorder in the filament bundle and the heterogeneity in the interface layer are described in form of statistical distributions. The correlation between these distributions is analyzed. Based on this analysis an approach to derive an objective statistical representation of the material structure is proposed. Finally the application to the experiment is described.

1 INTRODUCTION

Textile reinforced concrete (TRC) has emerged in the last decade as a new composite material combining the textile reinforcement with cementitious matrix. Its appealing feature is the possibility to produce filigree high-performance structural elements that are not prone to corrosion as it is the case for steel reinforced concrete. In comparison with other composite materials, textile reinforced concrete exhibits a high degree of heterogeneity and imperfections that requires special treatment in the development of numerical models.

In particular, the material structure at the micro scale exhibits high amount of irregularities and imperfections in the geometrical layout of the basic components with varying local properties and in the quality of local bindings between them. As an example, these imperfections may be represented by non-parallel orientation of filaments within the bundle or by varying bond quality between filaments and matrix across the bundle. As a result, the damage localization process of textile reinforced concrete exhibits interactions between elementary failure mechanisms in the matrix, in the reinforcement and in the bond.

The presence of imperfections in the yarn and in the bond structure makes it necessary to account for the effect of scatter of the material properties on the performance of the crack bridges. The crack bridges are the hot-spots of deformation and interaction of damage with localized damage at the material interfaces of matrix and reinforcement. In a way the crack bridge is equivalent to a tensile test on yarn with an extremely short length equipped with a shear-lag-like clamping of filaments. Due to the varying penetration profile

along the yarn, the quality of the shear lag clamping exhibits high scatter. What is sought is a true statistical representation of the material structure able to reproduce the crack bridge behavior in different configurations and loading histories.

The paper describes the construction of crack bridge models and shows several parametric studies classifying the influence of variations in filament and bond properties on the performance of the crack bridge.

2 APPROACHES TO MODELING CRACK BRIDGE BEHAVIOR

The filament bundle models provide the stepping stone for robust modeling of the failure process in the bond layer between the multifilament yarn and the cementitious matrix. In the following the existing models for cracks bridged by fibers or fiber bundles will be classified based on the considered variability of material parameters.

The effect of the irregular bond structure on the performance of the crack bridge has been represented by a distribution of the effective filament lengths in (Schorn 2003). (Banholzer 2004) additionally considers a finite bond and the abrasion of the filaments during the debonding. In (Lin et al. 1999) a micromechanical model has been developed to characterize the interfacial properties at single fiber pullout. The effect of fiber alignment on the pullout load was investigated in (Li 1992). The influence of fiber alignment on in-situ strength has been characterized in (Kanda and Li 1998). In (Lin et al. 1999) Eqn. (1) has been used to derive the crack bridging stress versus crack opening relation by averaging over the contributions of the fil-

aments.

With the strain based formulation of statistical fiber bundle model (Phoenix and Taylor 1973) it is possible to evaluate the mean response of the bundle under tensile loading analytically:

$$\mu_\theta(e) = \int_\theta q_e(e; \theta) dG_\theta(\theta). \quad (1)$$

Where $q_e(e, \theta)$ represents the filament constitutive law with global strain e and the vector of material parameters θ and $G_\theta(\theta)$ is the cumulative probability distribution function of the parameter(s) θ .

We note that this class of models is limited to the local load sharing between filaments upon filament break. In other words, the load of the lost filament gets uniformly distributed across the bundle. Based on the experimental evidence of low friction between filaments presented in (Chudoba, Konrad, Vořechovský, and Roye 2006) we neglect the interaction effect between the filaments with effective lengths the in range of several millimeters as they occur in the crack bridge.

A thorough study of sources of randomness/disorder in the multi-filament yarn that are relevant for its performance in textile reinforced concrete has been presented in (Chudoba et al. 2006). For the analysis of bundles with infinite number of fibers a continuous analytical model with refined kinematic relation has been developed. The considered distributions of material properties include both the variations of parameters from filament to filament and the variations of local strength and material stiffness across the bundle. In the companion paper (Vořechovský and Chudoba 2006) the variations of material properties over the length are considered.

The scatter of filament stiffness parameters leads to a reduced strength of a bundle with a very short length. In a crack bridge the strength reduction is in particular caused by the scatter of filament lengths and their delayed activation (slack). Besides that, the scatter of filament strength across the bundle leads to a further reduction of the bundle peak force (Smith and Phoenix 1981).

In order to demonstrate the effect on an example we consider a crack bridge with a scatter of filament lengths. In particular, we introduce the relative difference of the filament length with respect to the minimum length as $\lambda = (\ell_{\max} - \ell_{\min}) / \ell_{\min}$ with a uniform distribution, i.e. $G_\lambda(\lambda) = \lambda / \lambda_{\max}$ where $0 \leq \lambda \leq \lambda_{\max}$. The other parameters of the filament, i.e. Young's modulus E , area A and breaking strain ξ are considered constant. For the chosen distribution, it is possible to derive analytical formulas for the bundle mean strength and its variance (Chudoba et al. 2006)

at a given control strain e as

$$\begin{aligned} \mu_\lambda(e; \lambda) &= \int_\lambda q_e(e; \lambda) dG_\lambda(\lambda) \\ &= \begin{cases} EAe \ln(1 + \lambda_{\max}) / \lambda_{\max} & \text{for } 0 \leq e \leq \xi \\ EAe \frac{\ln(1 + \lambda_{\max}) - \ln(e/\xi)}{\lambda_{\max}} & \text{for } e \geq \xi \end{cases} \end{aligned} \quad (2)$$

The calculated mean load strain diagrams for a bundle with 1743 filaments and constant diameter $D = 25.5 \mu\text{m}$, Young's modulus $E = 70 \text{GPa}$ and breaking strain $\xi = 1.79\%$ are exemplified in Fig. 1 for several levels of scatter represented by λ_{\max} .

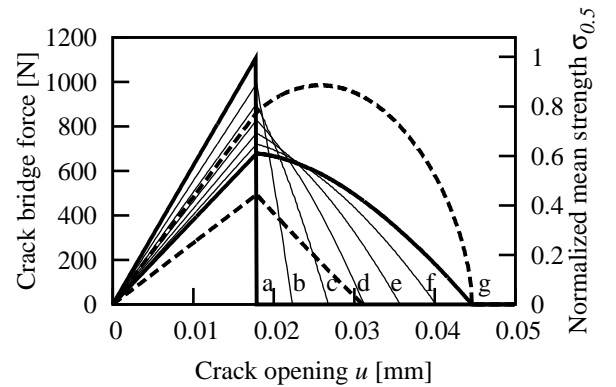


Figure 1: Mean load-displacement diagrams of one crack bridge with uniform distribution of additional fiber length $\lambda \in (0, \lambda_{\max})$. $\lambda_{\max} =$ a) 0.0, b) 0.25, c) 0.5, d) 0.75, e) 1.0, f) 1.25 and g) 1.5 plotted with a scatterband (mean \pm standard deviation).

The introducing example demonstrates the modeling concept used in the first part of this paper. In addition to the scatter of filament lengths, we shall include the scatter of the bond quality across the bundle. In order to justify this decision we first discuss the issue of appropriate choice of material parameters in general.

3 OBJECTIVITY OF THE MATERIAL PARAMETERS

The overall goal in the construction of the model of a crack bridge is to predict its performance in a broad application context, i.e. in an arbitrary configuration of cracks and textile fabrics. These configurations are represented by the crack spacing on the one hand and by the angle at which the roving crosses the crack on the other hand. In this paper we consider only tensile response and limit the discussion to the aspects of bond parameters that should be independent of crack spacing (Fig. 2).

The minimum number of structural parameters is given by their capability to reflect the changes in the material structure during the evolution of local damage. As shown in the example in Fig. 1, it is possible

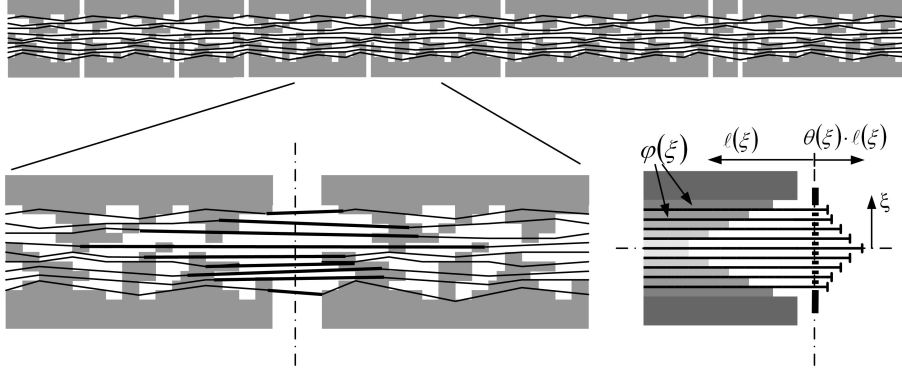


Figure 2: Heterogeneity in the material structure with the sought distributions of micromechanical parameters.

to find such a distribution of filament lengths that can reasonably reproduce the experimental response. Indeed, the performance of a single crack can be reproduced by a proper choice of length profile resulting in the corresponding number of breaks at each level of control displacement. However, this distribution of smeared effect of length and bond variations cannot be considered representative in the context of multiple cracks. There are especially two reasons:

- The crack bridge with structural variations ascribed solely to the effective length would exhibit a shorter stress transfer length than under the assumption of finite bond. Therefore the fitted crack bridge stiffness would not be consistent with the bond stiffness and, thus, inconsistent with the crack spacing.
- Even if the crack spacing would be defined a priori, e.g. using the experimentally measured crack distribution, the effective length profiles obtained from a single crack bridge experiment would lead to an underestimated stiffness in the case of unloading of existing cracks at the formation of a new crack. This is due to the fact the the stiffness reduction during the opening of a crack bridge can only be appointed to the failure of filaments. Therefore the crack will unload with the resulting secant stiffness. A consideration of plastic deformations in the interface leads to significantly higher stiffness.

Separate consideration of the scatter of lengths and of the bond quality across the bundle in the vicinity of a crack bridge allows us to capture interactions between cracks. It would certainly be possible to resolve the material structure in even more detail. On the other hand, a pragmatic material resolution requires only to capture the components and interfaces that dominate in the disintegration of the material structure.

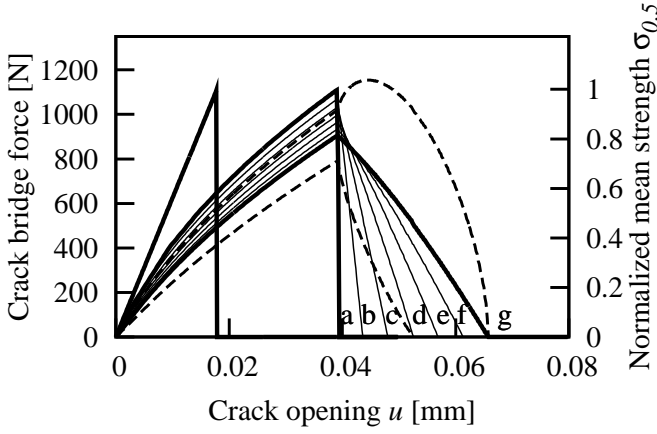
4 EFFECT OF FINITE BOND STRENGTH

The procedure for evaluating the total strength described in Sec. 2 can be used with more complex idealizations of a crack bridge taking into account further failure and damage mechanisms. In addition to filament rupture considered in the previous model we now include the influence of debonding between filament and matrix. The performance of a multifilament yarn bridging a crack is evaluated by replacing the constitutive law $q_e(e, \theta)$ in Eq. (1) with a filament pull-out response $p_u(u, \theta)$ that could be derived analytically using a shear lag model (Stang et al. 1990) with a cohesive interface between the filament and matrix.

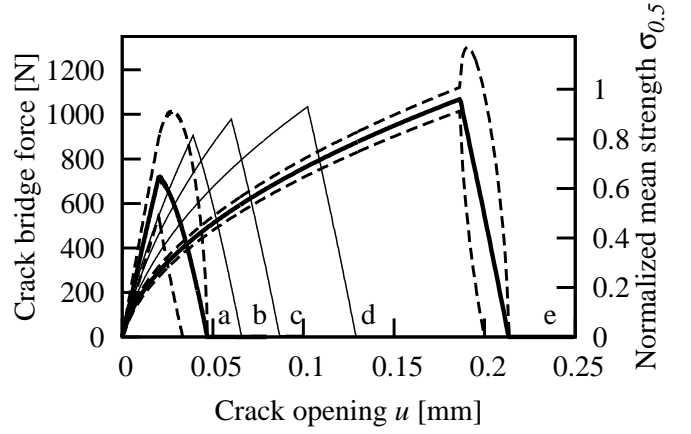
With $G_\lambda(\lambda)$ defined as in the last example, we now include the debonding of a filament from the matrix as an additional effect characterizing the interface between a perfectly embedded filament and the cementitious matrix. In (Banholzer 2004) filament matrix bond laws for perfectly embedded filaments have been derived as multi linear functions $\tau_1(s)$ (with s representing the slip) using the filament pull-out test and the cohesive interface model. In the particular case of the Vetrotex AR-glass roving with 2400 tex the derived function shows that no adhesional bond is developing and thus the interfacial properties are predominated by friction. Therefore $\tau_1(s)$ can be represented in the following bilinear form:

$$\tau_1(s) = \tau_{fr} \cdot \begin{cases} s/s_{crit} & 0 \leq s \leq s_{crit} \\ 1 & s \geq s_{crit} \end{cases} \quad (3)$$

Again we keep all other parameters including the interface characteristics, constant. Fig. 3.1 shows the load displacement diagrams for the varied range of lengths with $\lambda_{max} \in [0, 0.25, 0.5, 0.75, 1, 1.25, 1.5]$ and a constant bond stress $\tau_1 = 3.38$ MPa. It exemplifies that the crack opening at peak load increases due to the debonding of the filaments. To demonstrate this effect we now keep $\lambda_{max} = 1.5$ constant and vary the bond stress in the range $\tau_1 = c \cdot 3.38$ MPa,



3.1: $\tau_{fr} = 3.38$ MPa and $\lambda_{\max} =$ a) 0.0, b) 0.25, c) 0.5, d) 0.75, e) 1.0, f) 1.25 and g) 1.5 plotted with a scatterband (mean \pm standard deviation)



3.2: $\lambda_{\max} = 1.5$ and $\tau_{fr} = c \cdot 3.38$ MPa. $c =$ a) 10.0, b) 1.0, c) 0.5, d) 0.25, e) 0.125 plotted with a scatterband (mean \pm standard deviation)

Figure 3: Mean load-displacement diagrams of one crack bridge with debonding τ_{fr} and with uniform distribution of additional fiber length $\lambda \in (0, \lambda_{\max})$.

$c \in [10, 1, 0.5, 0.25, 0.125]$. The resulting load displacement diagram Fig. 3.2 shows that the mean crack bridge strength increases significantly with decreasing bond stress τ_1 .

The reason for this increased strength is the homogenizing effect of the debonding causing a more uniform stress distribution across the bundle (more filaments can act simultaneously before they break). We also note that there is a significant reduction in the scatter of strength compared to Fig. 3.1: 184 N for perfect bond and 50 N with included debonding and the lowest bond stress.

5 EFFECT OF SCATTER IN BOND STRENGTH

Due to the irregular penetration of the matrix into the yarn the quality of the interface between matrix and fillment varies. The reason for this scatter of bond quality are the varying contact area between filament and matrix and variations in the quality of the matrix itself due to the heterogeneous infiltration of aggregate particles. To evaluate the influence of the scatter in the interface we introduce the bond quality φ of an individual filament as a dimensionless scaling factor for the bond law. The bond stress slip relation for this filament in the bundle is defined as follows:

$$\tau(s, \varphi) = \varphi \tau_1(s) \quad (4)$$

The influence of a bond quality uniformly distributed over the bundle cross section with $G_\varphi(\varphi)$ and $\lambda_{\max} = 0$ (all filaments have the same bond free length) is exemplified in Fig. 4. The bond quality φ has significant influence on the stiffness. With decreasing mean bond quality μ_φ the stiffness decreases due to the large amount of debonding (Fig. 4.1. The peak load is reached at larger displacements. An increased scat-

ter (σ_φ) leads to reduced peak load and more ductile post peak behavior as a result of more inhomogenous stress transfer in the interface (Fig. 4.2).

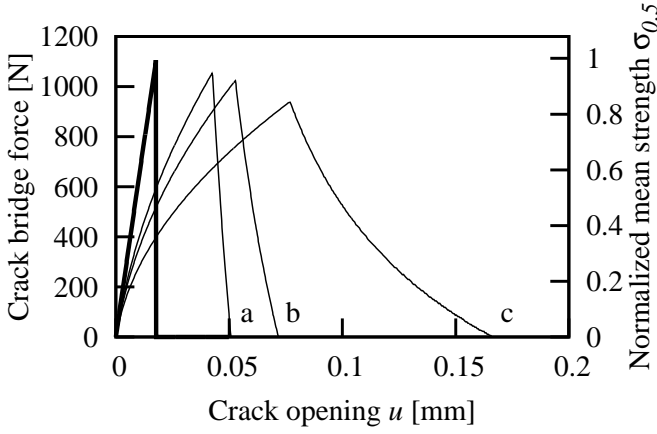
6 EFFECT OF CORRELATION

The micrographs in Fig. 5 suggest that there is a positional dependence for the two studied parameters ℓ and φ . Regarding the outside filaments of the cross section we see that they are very well embedded ($\varphi \approx 1$) while their free length is very short ($\lambda \approx 0$). For the inner filaments we can observe the opposite. This raises the question of correlation between these two random parameters. In order to evaluate the influence of this correlation we shall consider φ and λ normally distributed using the bivariate normal distribution:

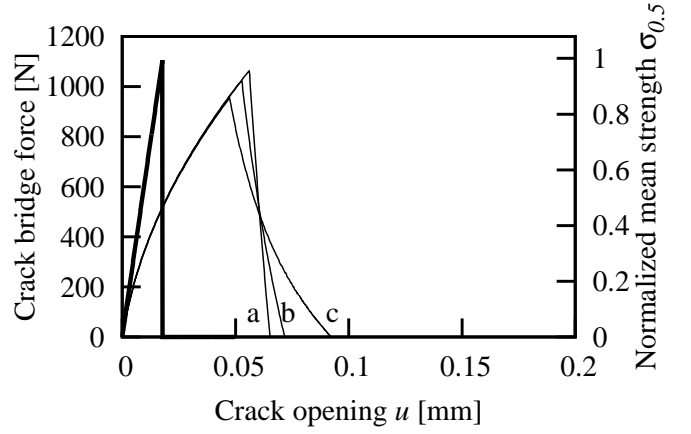
$$G(\varphi, \lambda) = \frac{e^{-\frac{z}{2 - 2\rho_{\varphi, \lambda}^2}}}{\pi \sigma_\varphi \sigma_\lambda \sqrt{1 - \rho_{\varphi, \lambda}^2}} \quad (5)$$

$$z = \frac{(\varphi - \mu_\varphi)^2}{\sigma_\varphi^2} - 2 \frac{\rho_{\varphi, \lambda} (\varphi - \mu_\varphi) (\lambda - \mu_\lambda)}{\sigma_\varphi \sigma_\lambda} + \frac{(\lambda - \mu_\lambda)^2}{\sigma_\lambda^2}$$

with $\rho_{\varphi, \lambda}$ standing for the correlation coefficient. Figs. 6 and 7 demonstrate that the qualitative effects

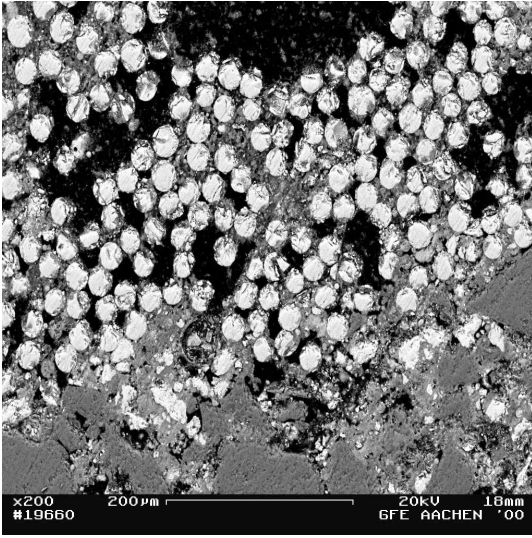


4.1: $\mu_{phi} =$ a) 0.75, b) 0.5, c) 0.25, $\sigma_{phi} = .125$

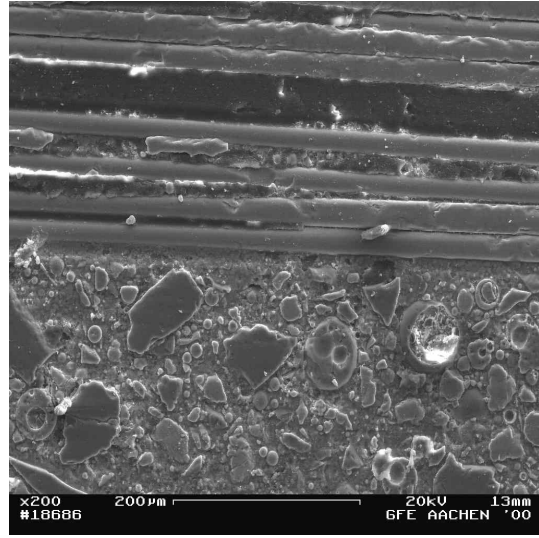


4.2: $\mu_{phi} = 0.5$, $\sigma_{phi} =$ a) 0.125, b) 0.0625, c) 0.03175

Figure 4: Mean load-displacement diagrams of one crack bridge with constant bond free length ($\lambda_{max} = 0$) and uniform distribution of bond quality $\varphi[-]$.



5.1: cross section



5.2: longitudinal section

Figure 5: SEM micrographs of a multifilament yarn embedded in the cementitious matrix.

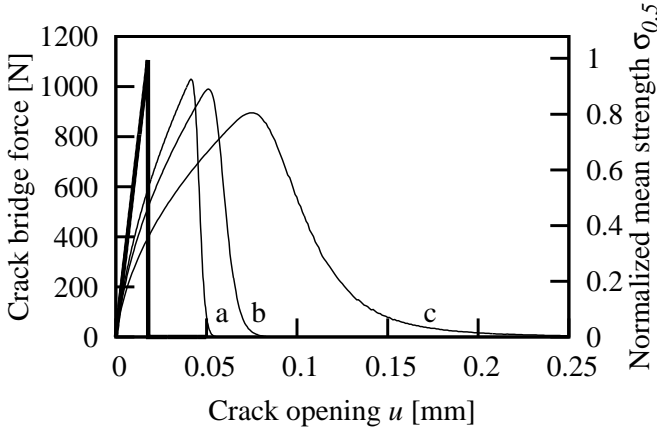
described in the sections above can be reproduced using normal distributions. The load strain diagrams show smoothed response at the peak load and at the tails due to the concentration of the normal distribution at the mean values.

The effect of the correlation between the bond quality φ and the bond free length $\lambda \cdot \ell_{min}$ is demonstrated in Fig. 8 for a correlation coefficient $\rho_{\varphi,\lambda} \in (-1, 1)$. The correlation coefficient $\rho_{\varphi,\lambda} = 0$ indicates that φ and λ are completely independent. For $\rho_{\varphi,\lambda} = 1$ the minimum values of φ coincide with the minimum values of λ for $\rho_{\varphi,\lambda} = -1$ the minimum values of φ coincide with the maximum values of λ . A strong negative correlation (Fig. 8 a): $\rho_{\varphi,\lambda} \approx -1.0$ leads to a slightly reduced crack bridge performance. The negative correlation leads to more inhomogeneous stress trans-

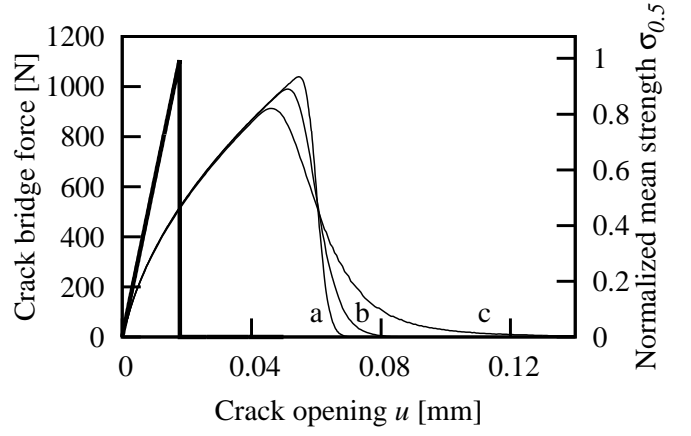
fer reducing the peak load and associate crack opening to higher stress in the softening branch. This corresponds to the combination of short filaments with high bond and long filaments with low bond. We remark if it would be technically possible to achieve the other extreme and combine low bond quality with large bond free lengths and vice versa, it would be possible to obtain an increased bond performance.

7 APPLICATION TO THE EXPERIMENT

In order to relate the discussed issues to experimental data we shall identify the parameters characterizing the material structure using a pull-out experiment. We shall simplify the model in such a way that the variability is considered only deterministically. This is justified by relatively low effect of correlation dis-



7.1: $\mu_{phi} =$ a) 0.75, b) 0.5, c) 0.25, $\sigma_{phi} = .125$



7.2: $\mu_{phi} = 0.5$, $\sigma_{phi} =$ a) 0.125, b) 0.0625, c) 0.03175

Figure 7: Mean load-displacement diagrams of one crack bridge with constant bond free length ($\lambda_{max} = 0$) and normal distribution of bond quality $\varphi[-]$.

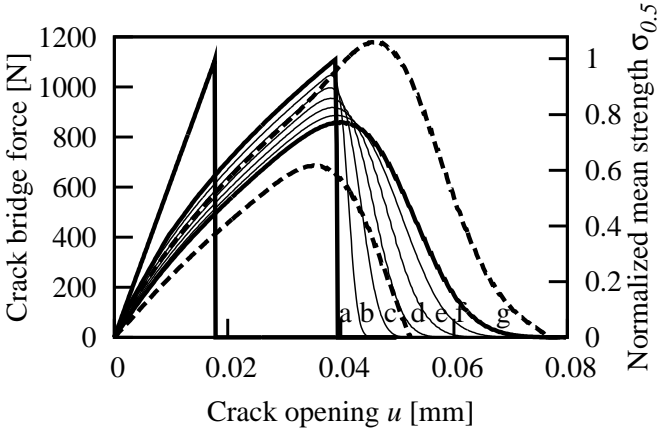


Figure 6: Mean load-displacement diagrams of one crack bridge with debonding (τ_{fr} [MPa] = 3.38) and normal distribution of additional fiber length $\lambda \in (0, \lambda_{max})$. $\lambda_{max} =$ a) 0.0, b) 0.25, c) 0.5, d) 0.75, e) 1.0, f) 1.25 and g) 1.5 plotted with a scatterband (mean \pm standard deviation).

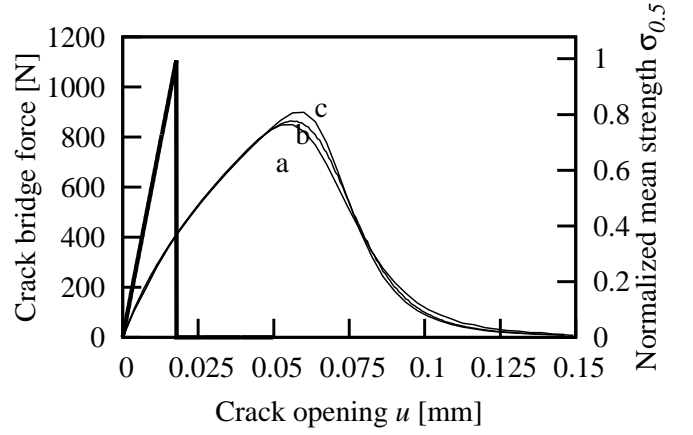


Figure 8: Effect of correlation between bond free length and bond quality ($\rho_{\varphi,\lambda} =$ a) -0.99, b) 0.0, c) 0.99).

cused above. If we assume $\rho_{\varphi,\lambda} \rightarrow -1.0$ we can interpret the inverse cumulative density functions of our distributions as profiles of heterogeneity varying across the bundle with the random nature replaced by the parametric coordinate ξ (Fig. 9) representing the position of the filament in the bundle.

Based on numerical and experimental studies and for the sake of completeness we introduce the third parameter considered in the model: The delayed activation of filaments (slack) within the bond free length. We further assume negative correlation between bond quality and delayed activation. The interaction of the delayed activation with the bond free length and the bond quality has been described by (Konrad and Chudoba 2004).

For the purpose of numerical calibration using the experimental data we approximate the introduced

profiles by the following polynomial functions:

$$\begin{aligned} \varphi(\xi) &= (k_{\varphi,0} + k_{\varphi,1} - 2) \xi^3 \\ &- (3 - 2k_{\varphi,0} - k_{\varphi,1}) \xi^2 \\ &+ k_{\varphi,0} \xi \end{aligned}$$

$$\lambda(\xi) = \lambda_{max} + (\lambda_{min} - \lambda_{max}) \xi \quad (6)$$

$$\begin{aligned} \theta(\xi) &= (2\theta_{max} - k_{\theta,1}) \xi^3 \\ &+ (2k_{\theta,1} - 3\theta_{max}) \xi^2 \\ &+ k_{\theta,1} \xi + \theta_{max} \end{aligned}$$

The parametric coordinate $\xi = 0$ represents the idealized center of the bundle and $\xi = 1$ coincides with the outer layer of the bundle.

With the assumption of uniform distribution of imperfections in the bond and yarn structure along the specimen the effect of imperfection on the performance of each crack bridge can be considered the same. Thus, the quantification of this effect can be performed with an isolated analysis of a pull-out experiment in connection with the bond layer model

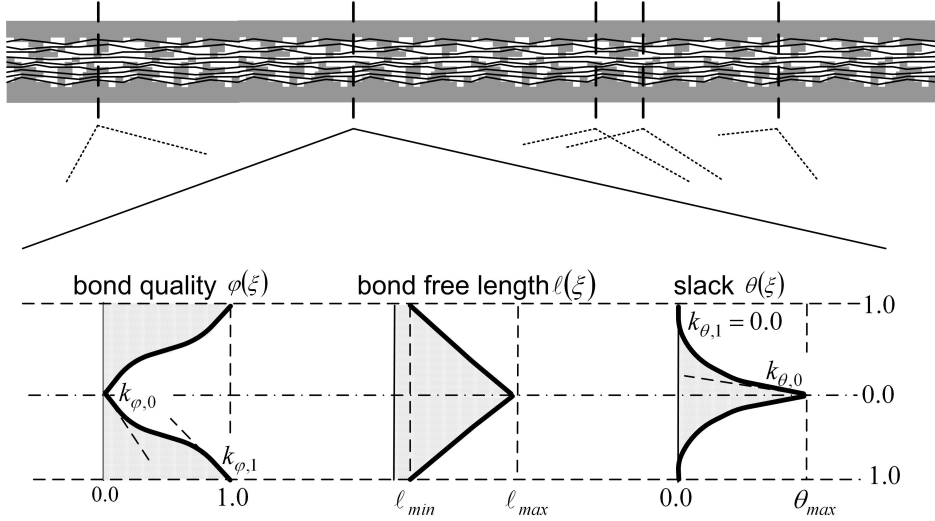


Figure 9: Profiles describing the heterogeneity in the material structure.

shown in Fig. 2. As can be seen in the figure the profiles of heterogeneity are directly used for discrete representation of the crack bridge. We emphasize that the fine resolution of the material structure further away from the crack bridge is not needed due to the increasingly homogeneous stress profile.

In this way we construct the discrete bond layer model (Fig. 2) with the interface layer between the yarn and the matrix represented by a set of laminas. Each lamina interacts with the matrix through a given bond law. It represents a subset of filaments with the same characteristics and is coupled with the matrix using zero thickness interface elements (Kaliakin and Li 1995).

The bond law distributed over the bond layer is then constructed as:

$$\tau(s, \xi) = \tau_1(s(\xi)) \varphi(\xi) \quad (7)$$

Equipped with the boundary conditions of a pull-out test the calibration (Chudoba et al. 2004) of the model is performed both using the load-displacement curve and the curve representing the instantaneous fraction of the unbroken filaments during the loading process. The latter is obtained experimentally using the FILT test (Failure Investigation using Light Transmission properties) by optical recording of the light transmission through the unbroken filaments (Banholzer 2004) (Fig. 10).

The parameters describing the profiles are obtained using the calibration framework of automated calibration procedures based on evolutionary strategies to avoid convergence to local minima.

8 SUMMARY

A specific feature of the textile reinforced concrete is the high degree of heterogeneity of the reinforcement and of the matrix on similar scales of the material structure. The complex damage and failure process

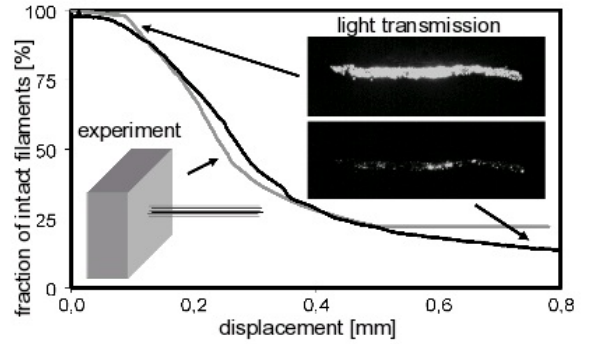


Figure 10: FILT-Test.

calls for an application of stochastic and micromechanical models that can reflect the heterogeneity.

In this paper a statistical fiber bundle model for the evaluation of the mean performance of a crack bridged by a multifilament yarn has been introduced. The effect of the disorder in the filament bundle has been described in form of distributions of relative extra filament length λ . We have shown that the scatter of filament lengths leads to a reduced performance of the crack bridge. The introduction of a finite bond strength has a homogenizing effect leads to an increasing strength at larger displacements. The heterogeneity of the interface layer was represented in form of a statistical distribution of bond quality φ . Increased scatter of the bond quality leads to reduced crack bridge strength performance. The negative correlation of variations in the bond quality φ and in filament lengths λ amplifies both effects. We have proposed an approach to deriving an objective statistical representation of the material structure using cross section profiles of the described parameters and have introduced a model utilizing these profiles. Finally, the evaluation of the material parameters calibrating the introduced model with experimental data has been described.

ACKNOWLEDGMENTS

The authors thank the German research foundation (DFG) in context of the Collaborative Research Center 532 for their financial support.

REFERENCES

- Banhöfer, B. (2004). *Bond Behaviour of a Multi-Filament Yarn Embedded in a Cementitious Matrix*. Ph. D. thesis, Institute for Building Materials Research, RWTH Aachen University.
- Chudoba, R., C. Butenweg, and F. Peiffer (2004). Technical information system for collaborative material research. *Advances in Engineering Software*, 747–756.
- Chudoba, R., M. Konrad, M. Vořechovský, and A. Roye (2006). Numerical and experimental study of imperfections in the yarn and its bond to cementitious matrix. *American Concrete Institute (ACI) Symposium Publication*.
- Chudoba, R., M. Vořechovský, and M. Konrad (2006). Stochastic modeling of multi-filament yarns I: Random properties within the cross section and size effect. *International Journal of Solids and Structures* 43(3-4), 413–434.
- Kaliakin, V. N. and J. Li (1995). Insight into deficiencies associated with commonly used zero-thickness interface elements. *Computers and Geotechnics* 17(2), 225–252.
- Kanda, T. and V. Li (1998). Interface property and apparent strength of a high strength hydrophilic fiber in cement matrix. *ASCE Journal of Materials in Civil Engineering* 10(1), 5–13.
- Konrad, M. and R. Chudoba (2004). The influence of disorder in multifilament yarns on the bond performance in textile reinforced concrete. *Acta Polytechnica, Band 44 , No. 5-6, Seiten 186-193, 2004*.
- Li, V. (1992). Post-crack scaling relations for fiber reinforced cementitious composites. *ASCE Journal of Materials in Civil Engineering* 4(1), 41–57.
- Lin, Z., T. Kanda, and V. C. Li (1999). On interface property characterization and performance of fiber-reinforced cementitious composites. *Concrete Science and Engineering* 1, 173–184.
- Phoenix, S. L. and H. M. Taylor (1973). The asymptotic strength distribution of a general fiber bundle. *Advances in Applied Probability* 5, 200–216.
- Schorn, H. (2003). Ein verbundmodell für glasfaserbewehrungen im beton. *Bautechnik* 80(3), 174–180.
- Smith, R. L. and S. L. Phoenix (1981, 3). Asymptotic distributions for the failure of fibrous materials under series-parallel structure and equal load-sharing. *Journal of Applied Mechanics* 48, 75–82.
- Stang, H., Z. Li, and S. P. Shah (1990). Pull-out problem: Stress versus fracture mechanical approach. *Journal of Engineering Mechanics* 116(10), 2136–2150.
- Vořechovský, M. and R. Chudoba (2006). Stochastic modeling of multi-filament yarns II: Random properties over the length and size effect. *International journal of Solids and Structures* 43(3-4), 435–458.